

Indole-Containing Pyrazino[2,1-*b*]quinazoline-3,6-diones Active against *Plasmodium* and Trypanosomatids

Published as part of the ACS Medicinal Chemistry Letters virtual special issue “Medicinal Chemistry in Portugal and Spain: A Strong Iberian Alliance”.

Solida Long, Denise Duarte, Carla Carvalho, Rafael Oliveira, Nuno Santarém, Andreia Palmeira, Diana I. S. P. Resende, Artur M. S. Silva, Rui Moreira, Anake Kijjoa, Anabela Cordeiro da Silva, Fátima Nogueira,* Emília Sousa,* and Madalena M. M. Pinto



Cite This: <https://doi.org/10.1021/acsmchemlett.1c00589>



Read Online

ACCESS |



Metrics & More



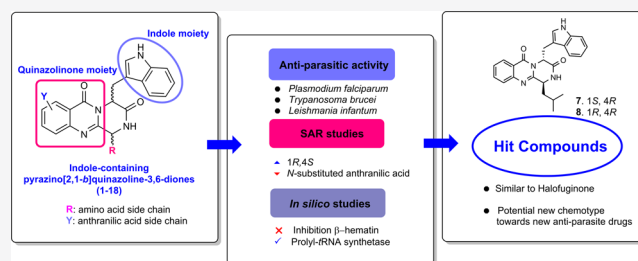
Article Recommendations



Supporting Information

ABSTRACT: Malaria, leishmaniasis, and sleeping sickness are potentially fatal diseases that represent a real health risk for more than 3,5 billion people. New antiparasitic compounds are urgent leading to a constant search for novel scaffolds. Herein, pyrazino[2,1-*b*]quinazoline-3,6-diones containing indole alkaloids were explored for their antiparasitic potential against *Plasmodium falciparum*, *Trypanosoma brucei*, and *Leishmania infantum*. The synthetic libraries furnished promising hit compounds that are species specific (7, 12) or with broad antiparasitic activity (8). Structure–activity relationships were more evident for *Plasmodium* with anti-isomers (1*S*,4*R*) possessing excellent antimalarial activity, while the presence of a substituent on the anthranilic acid moiety had a negative effect on the activity. Hit compounds against malaria did not inhibit β -hematin, and *in silico* studies predicted these molecules as possible inhibitors for prolyl-tRNA synthetase both from *Plasmodium* and *Leishmania*. These results disclosed a potential new chemotype for further optimization toward novel and affordable antiparasitic drugs.

KEYWORDS: Pyrazino[2,1-*b*]quinazoline-3,6-dione, antimalarial, *P. falciparum*, *Leishmania*, *Trypanosoma brucei*



Parasitic diseases such as malaria, leishmaniasis, and trypanosomiasis affect billions of people, being responsible for almost half a million fatalities per year.^{1–4} Although vaccines for leishmaniasis and trypanosomiasis are still not available, several vaccine candidates, with different modes of action, are in various stages of development to prevent *Plasmodium falciparum* and *P. vivax* infections.¹ The European Medicines Agency released a positive scientific opinion in 2015 about RTS,S/AS01, which enabled a pilot implementation of this vaccine in some African countries in 2019.¹ Recently, the World Health Organization (WHO) recommended that this vaccine may be used for the prevention of *P. falciparum* malaria in children living in regions with moderate to high transmission.⁴ The lack of vaccines to prevent the fatalities associated with parasitic diseases, associated with the fact that common chemotherapies are usually suboptimal, lead to growing concerns related to the emergence of resistance.^{1–4} Malaria is an infectious tropical disease caused by a unicellular and intracellular eukaryotic protozoan parasite belonging to the genus *Plasmodium*.⁵ There are five species identified that cause human malaria, namely, *P. falciparum*, *P. vivax*, *P. malariae*, two subspecies of *P. ovale* (*P. ovale curtisi* and *P. ovale wallikeri*), and *P. knowlesi*.⁶ *P. falciparum* and *P. vivax* are the

most predominant and represent the majority of the global malaria cases, with *P. falciparum* being the most virulent species of human malaria.⁶ The WHO Global technical strategy for malaria 2016–2030, updated in 2021, sets ambitious but achievable global targets, including the reduction of malaria case incidence and mortality rates by at least 90% by 2030.¹ Nonetheless, in the 2021 malaria report, the WHO estimated 14 million more malaria cases and 47 000 more deaths in 2020 compared to 2019, due to disruptions to services during the COVID-19 pandemic.⁴ The milestones of WHO’s global malaria strategy have been missed, and without immediate and dramatic action the 2030 targets will not be met.⁴ Evidence of a multidrug-resistant *P. falciparum* parasite lineage in some countries in Southeast Asia especially at Greater Mekong Subregion (GMS), including the Lao People’s

Received: October 25, 2021

Accepted: January 7, 2022

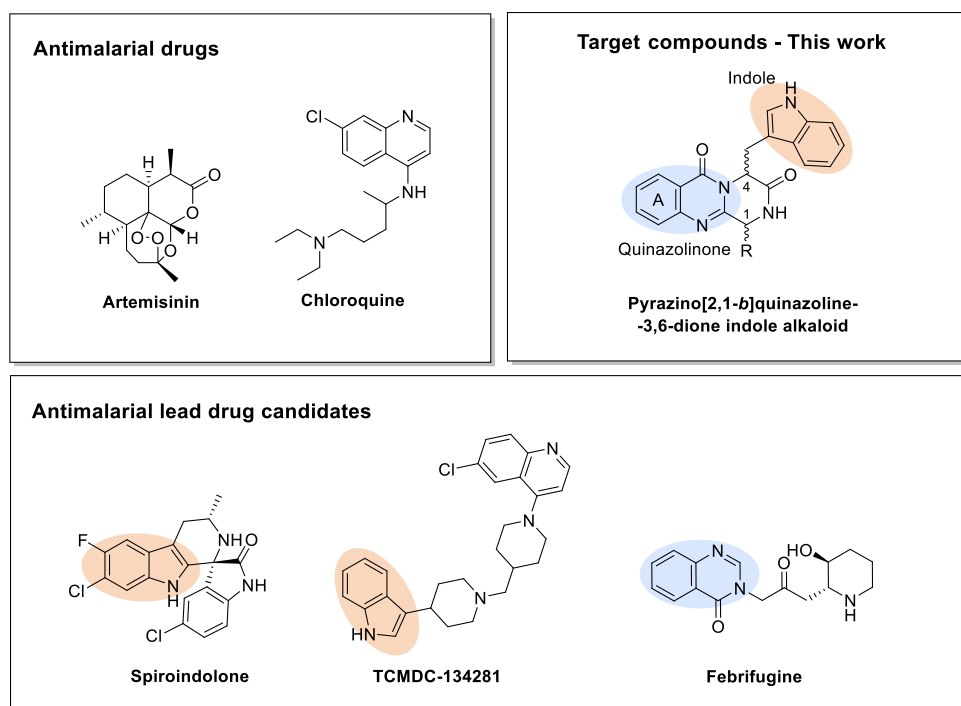


Figure 1. Current antimalarial drugs artemisinin and chloroquine, indole containing antimalarial compounds spiroindolone and TCMDC-134281, natural antimalarial compound febrifugine, and scaffold of the target compounds 1–28, an indole-containing pyrazino[2,1-*b*]quinazoline-3,6-dione.

Democratic Republic, Thailand, Cambodia, Myanmar, and Vietnam,⁴ represents a serious threat to global malaria control and eradication. The frontline therapies for the treatment of symptomatic malaria are artemisinin combination therapies (ACTs) for *P. falciparum* infections and chloroquine (CQ), or ACTs are usually employed for infections with *P. vivax*. However, these strategies were not so effective due to the slower parasite clearance cases that were observed.⁷ This evidence, along with widespread resistance to existing antimalarial drugs, shows the need to identify new chemical structures, ideally with novel antimalarial modes of action.

Leishmaniasis is the generic name of a group of neglected diseases (ND) caused by *Leishmania* sp., transmitted to humans by infected female sandflies. The three most significant forms of leishmaniasis are cutaneous (CL), mucocutaneous (ML) and visceral (VL). The latter is the most severe form, characterized by fever episodes, loss of weight, anemia, and hepatosplenomegaly. VL is highly widespread in the Indian subcontinent and in East Africa, where an estimated 200 000–400 000 new cases occur each year, being also prevalent in the Mediterranean basin (Portugal, Spain, Greece, and Italy), and South America.² In fact, leishmaniasis is also a major health issue and a social problem. There is the global commitment as stated by the 2012 London Declaration on Neglected Tropical Diseases to eradicate this disease.

Human African trypanosomiasis (HAT) or sleeping sickness is a potentially fatal disease caused by two trypanosome species reported in different areas, *Trypanosoma brucei gambiense* in West and Central Africa and *Trypanosoma brucei rhodesiense* in East Africa.⁸ Prone to fatal epidemic outbreaks that killed thousands, this disease has been controlled due to accessibility to new drugs. This led to its enclosure in the WHO Roadmap for extermination, elimination, and control of neglected tropical diseases.³

From a drug-development perspective, Nature is a reservoir for providing antiparasitic drugs because (1) malarial chemotherapy has always been successfully isolated from natural products and natural product mimetics, (2) the latest advanced technologies are now conveying issues associated with natural product discovery, and (3) functional group diversities from synthetic analogues and scaffold platforms engineered into living organisms during biosynthesis continue to provide biologically active mimics and selective ligands for cellular targets.⁹ From this point of view, approaches used for the development of novel antiparasitic drugs include the discovery of new active molecules from natural products,⁹ regeneration of existing drug, development of hybrid compounds,¹⁰ and rational drug design with chemical modifications of existing drugs and hits.¹¹

Screening of the recently publicized Tres Cantos Antimalarial Set (TCAMS) of GlaxoSmithKline (GSK)¹² suggested that the next generation of antimalarial drugs should include compounds bearing an indole group. This functional group is known to be an essential fragment in several lead drug candidates expressing new mechanisms of action, such as the spiroindolone and aminoindole derivatives.^{13,14} For example, TCMDC-134281 exhibited very potent antiparasitodal properties against the *P. falciparum* 3D7 strain ($EC_{50} = 34$ nM).¹⁵ However, although this compound showed no significant cytotoxicity against the human HepG2 hepatoma cell line ($EC_{50} > 10$ μ M), the presence of the 4-aminoquinolyl fragment (an essential pharmacophore of CQ) might be responsible for cross-resistance with CQ and poor druglike properties.

Indole-containing pyrazino[2,1-*b*]quinazoline-3,6-diones (Figure 1) constitute a subclass of alkaloids mostly isolated from marine and terrestrial sources.^{16,17} These structurally unique alkaloids contain simultaneously a quinazoline core which can be found in the structure of the natural febrifugine

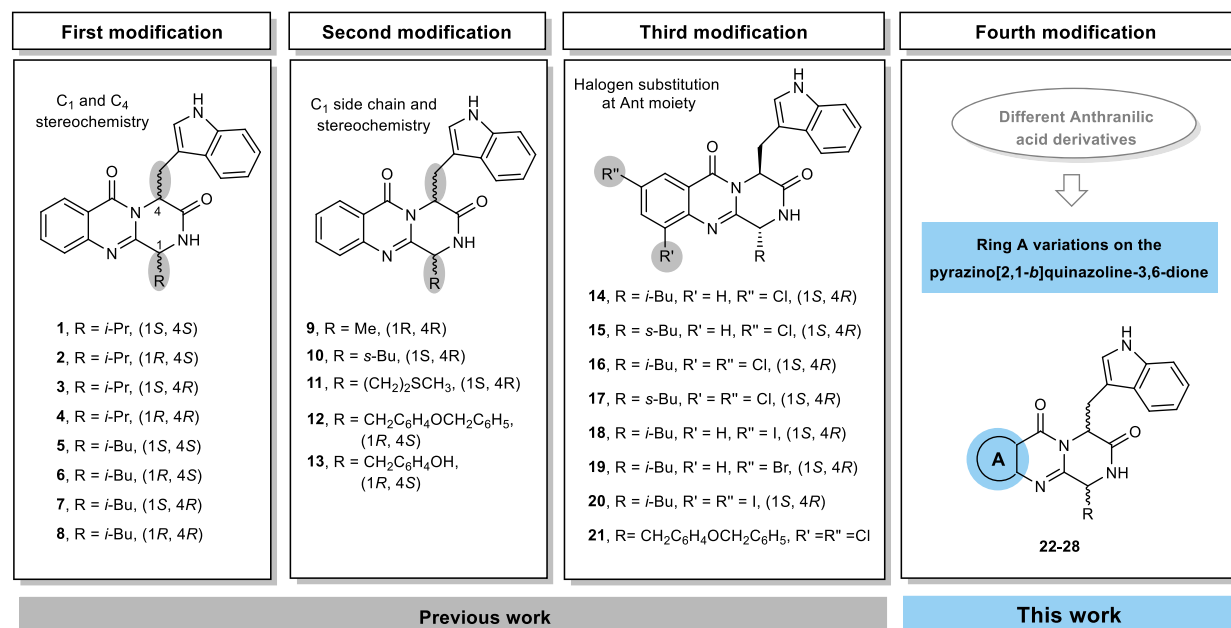


Figure 2. Structures of the four series of indole-containing pyrazino[2,1-*b*]quinazoline-3,6-diones 1–28 investigated in this study.

and an indole moiety commonly found in several drug lead candidates such as spiroindolone and TCMDC-134281 (Figure 1). This hybrid structure, containing both moieties, led us to hypothesize the antimalarial potential of derivatives with this scaffold and their ability to overcome the observed cross-resistance with CQ and ACTs (Figure 1). In previous works, three series of derivatives were built aiming to explore the chemical and biological space of indole-containing pyrazino[2,1-*b*]quinazoline-3,6-diones, with three molecular changes to naturally occurring fiscalins (Figure 2): (1) C-1 and C-4 stereochemistry modifications;¹⁸ (2) C-1 side chain and stereochemistry variation;¹⁹ and (3) introduction of halogen atoms in the aromatic ring of anthranilic acid.²⁰ In the present study, we explored these series and a fourth series consisting of ring A variations on the pyrazino[2,1-*b*]quinazoline-3,6-dione scaffold or with an additional indole moiety (Figure 2). The four series (compounds 1–28) were assayed against the CQ-sensitive *P. falciparum* 3D7 strain. Since febrifugine-related compounds are promising antiparasitic candidates, compounds were further investigated against *T. brucei* and *L. infantum*. New indole-containing pyrazino[2,1-*b*]quinazoline-3,6-diones 22–28 were synthesized via a highly effective and environmentally friendly microwave-assisted multicomponent polycondensation of amino acids.²¹ This methodology allowed us to prepare the fourth series of pyrazinoquinazoline alkaloids through treatment of the anthranilic acid (i) derivatives with *N*-Boc-L-amino acids (ii) under classic heating conditions (55 °C, 16–24 h). Further addition of D-tryptophan methyl ester hydrochloride (iii) and the use of microwave irradiation (300 W, 220 °C, 1.5 min) allowed us to obtain the targeted products 22–28 (Table 1). The low yields (1–12%, Figure 2) of this one-pot reaction can be attributed to the high temperature applied in the last step, essential to convert the intermediate Boc-protected-benzoxazin-4-one to the final products.¹⁸ The steric hindrance at C-1 could also be a reason, as previously noted by Liu et al.²¹ This methodology was characterized by producing partial epimerization; the enantiomeric ratios of compounds 22–28 were determined by HPLC to be in the

range of 30–47:53–70, with the exception of 28, that presented an enantiomeric ratio of 99:1, probably due to the steric hindrance of the tryptophan moiety at C-1 (Figure 2).

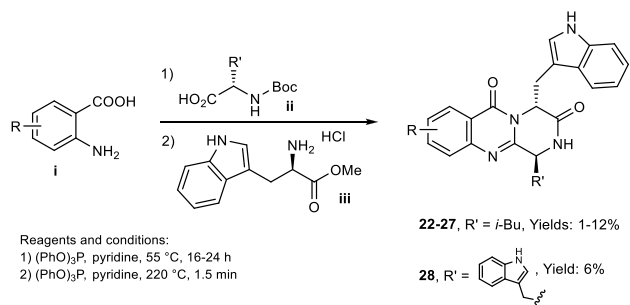
Twenty-eight quinazolinones consisting of 21 compounds of the first three series (1–21) and seven compounds from the fourth series (22–28) were tested for investigating their antiparasitic activity using distinct *in vitro* models for three different diseases malaria, leishmaniasis, and sleeping sickness.

The principles of the *in vitro* susceptibility tests are distinct, but they aim to evaluate, in biologically relevant settings, the activity of the compounds. In this context, for malaria, the readout was to assess the degree of development of parasites *P. falciparum* with different concentrations of compounds (Table 2). Regarding the assays related to the sleeping sickness, *T. brucei* bloodstream forms were used and for leishmaniasis evaluation intracellular *L. infantum* amastigotes was considered the relevant model to be used in this assay (Table 3).

To evaluate the antiparasitic potential of the indole-containing pyrazino[2,1-*b*]quinazoline-3,6-diones scaffold, our first approach was to screen the first series of compounds (1–8), having four types of stereoisomers (Figure 2). We observed that anti-isomers (1S,4R) (e.g., 3 and 7) exhibited the highest antimalarial activity while *syn*-isomers (1S,4S) were inactive (1 and 5). When compared to the obtained results for the anti-isomers, the *syn*-isomers (1R,4R) showed a decreased in activity (4 and 8). For *T. brucei syn* isomers, 1, 4, and 8 were the most active; this last compound was also active on *Leishmania*, suggesting a distinct isomer preference than *Plasmodium*. Compound 7, having an isobutyl group at C-1, demonstrated higher antimalarial activity than 3 with an isopropyl group at the same position, which might indicate that increasing the size of C-1 can lead to an improved antimalarial activity. The same trend was evident for *Leishmania* and *T. brucei*, with 8 being more active than 4.

To further evaluate the effect of C-1 substituent on the activity, the second series of compounds (9–13) was evaluated, and structure–activity relationship (SAR) studies indicate that a sulfur substituent at C-1 does not favor activity

Table 1. Microwave-Assisted Multicomponent Synthesis of Fourth Series Indole-Containing Quinazolinone Alkaloids 22–28



Anthranilic acid	Product	Compound	Yield ^(a) / <i>er</i> ^(b)
		22	6.9/47:53
		23	3.1/42:58
		24	5.8/30:70
		25	9.4/46:54
		26	12.1/46:54
		27	1.0/47:53
		28	5.7/99:1

^aObtained after purification. ^bDetermined by enantioselective liquid chromatography.

(compound 11). From this series, no compound was active against *Leishmania* while 12 was active against *T. brucei*. For the third series of compounds (14–21) with different substituents on the A ring, only compound 26 having a chlorine atom at position 9 and 11 showed favorable antimalarial activity with an IC₅₀ value of 0.2 μM (weaker than compounds 8 and 7), while other derivatives (substituted with Br or I) were shown to be inactive. These results correlate with other studies highlighting the effect of halogen substituents.²² For *T. brucei*, the A ring substitutions with electronegative groups like (Cl, Br, I, or OH) originated active compounds with similar activity profiles (16–19 and 22). Unlike the trend for *Plasmodium*, for *Leishmania*, only the Br and I derivatives (18 and 19) were active among the compounds from the third series. For the fourth series of indole-containing pyrazino[2,1-*b*]quinazolinone-3,6-dinones (22–28), isosteric substitutions with the nitrogen atom at

Table 2. *In Vitro* Activity against *P. falciparum* 3D7 Strain of Compounds 1–28 and Selectivity Index (SI) of Hit Compounds 3, 7, and 16

compd	<i>P. falciparum</i> (strain 3D7)		selectivity index ^d
	IC ₅₀ (μM) ^a ± SD ^b	LD ₅₀ (μM) ^c ± SD ^a	
1	>10	N.A. ^e	
2	>10	N.A. ^e	
3	0.10 ± 0.02	1.91 ± 0.44	19
4	0.15 ± 0.05	N.A. ^e	
5	>10	N.A. ^e	
6	2.00 ± 0.32	N.A. ^e	
7	0.05 ± 0.02	1.78 ± 0.47	34
8	0.47 ± 0.22	N.A. ^e	
9	3.68 ± 0.62	N.A. ^e	
10	>10	N.A. ^e	
11	>10	N.A. ^e	
12	>10	N.A. ^e	
13	4.18 ± 0.03	N.A. ^e	
14	>10	N.A. ^e	
15	>10	N.A. ^e	
16	0.20 ± 0.14	14.00 ± 1.41	70
17	1.51 ± 0.53	N.A. ^e	
18	>10	N.A. ^e	
19	>10	N.A. ^e	
20	>10	N.A. ^e	
21	4.00 ± 0.02	N.A. ^e	
22	0.73 ± 0.07	N.A. ^e	
23	>10	N.A. ^e	
24	>10	N.A. ^e	
25	4.00 ± 0.02	N.A. ^e	
26	3.76 ± 0.60	N.A. ^e	
27	1.02 ± 0.27	N.A. ^e	
28	>10	N.A. ^e	
CQ	0.1508 ± 0.0008	167.00 ± 42.00	11 074

^aIC₅₀: concentration that inhibits 50% growth of *P. falciparum* parasite (strain 3D7); ^bSD: standard deviation; ^cLD₅₀: lethal dose required to kill 50% of V79 mammalian cells; ^dSI: selectivity index, calculated by LD₅₀/IC₅₀. ^eN.A.: not active.

two different positions of the ring A (positions 10 and 11) led to decreased/abolished antimalarial activity (25 and 26). Compounds 22 and 24 each bearing a hydroxy or methoxy group at position 9 of ring A also showed a decrease in activity. Contrary to other reports of febrifugine derivatives,^{23,24} compound 27 with a tetrazole group at position 10 also showed weak activity against *P. falciparum*. This fourth series was also not active against *T. brucei* and *Leishmania*.

An important criterion in the evaluation of active compounds is their cytotoxicity in a mammalian host. In this context, the methylthiazolyl diphenyl-tetrazolium bromide (MTT) assay was used with different cells types. THP1 cells were used for primary general toxicity evaluation, while V79 cells from a nontumor cell line of Chinese hamster lung fibroblasts were also used for the most promising antimalarial hits, 3, 7, and 16.²⁵ The SARs from the first series of compounds suggest that a bigger C-1 substituent in conjugation with *syn*-isomerism is associated with cytotoxicity; in fact, 5 and 8 are the most toxic compounds from this first series. Compounds from the second series presented mixed cytotoxic profiles, and A ring substitutions in the third series lead to some toxicity, without evident SAR. Compounds from

Table 3. IC₅₀ Values of Compounds 1–28 against Leishmaniasis and Sleeping Sickness^a

compd	THP1		<i>T. brucei</i>		<i>L. infantum</i>	
	CC ₅₀ μM (95% CI)	IC ₅₀ μM (95% CI)	selectivity index (CC ₅₀ /IC ₅₀)		IC ₅₀ μM (95% CI)	selectivity index (CC ₅₀ /IC ₅₀)
1	>100	4.6 (4.4, to 4.8)	SI > 21.7		N.A. ^b	
2	>100	N.A. ^b			N.A. ^b	
3	>100	N.A. ^b			N.A. ^b	
4	>100	7.1 (6.8 to 7.5)	SI > 14.1		N.A. ^b	
5	50 < CC ₅₀ < 100	N.A. ^b			N.A. ^b	
6	>100	N.A. ^b			N.A. ^b	
7	>100	N.A. ^b			N.A. ^b	
8	25 < CC ₅₀ < 50	0.38 (0.36 to 0.41)	65.7 < SI < 131.5		2.6 (2.1 to 3.2)	9.6 < SI < 19.2
12	>100	1.6 (1.5 to 1.8)	SI > 62.5		N.A. ^b	
13	>100	N.A. ^b			N.A. ^b	
16	25 < CC ₅₀ < 50	5.9 (5.5 to 6.3)	4.2 < SI < 8.5		N.A. ^b	
17	50 < CC ₅₀ < 100	5.8 (5.5 to 6.0)	8.6 < SI < 17.2		N.A. ^b	
18	50 < CC ₅₀ < 100	4.1 (3.9 to 4.3)	12.2 < SI < 24.4		7.4 (5.3 to 10.5)	6.7 < SI < 13.5
19	50 < CC ₅₀ < 100	5.3 (5.1 to 5.6)	9.4 < SI < 18.9		7.8 (4.9 to 12.4)	6.4 < SI < 12.8
21	>100	3.9 (3.7 to 4.0)	SI > 25.6		N.A. ^b	
22	>100	8.6 (8.0 to 9.3)	SI > 11.6		N.A. ^b	
23	>100	N.A. ^b			N.A. ^b	
24	>100	N.A. ^b			N.A. ^b	
25	>100	N.A. ^b			N.A. ^b	
26	>100	N.A. ^b			N.A. ^b	
27	>100	N.A. ^b			N.A. ^b	
27	50 < CC ₅₀ < 100	N.A. ^b			N.A. ^b	
pentamidine	>10	2.2 ^c (1.9 to 2.5)	SI > 5000		N.A. ^b	
miltefosine	28.8 (24.2 to 34.2)	N.A. ^b			1.0 (0.8 to 1.2)	28.8

^aPresented data are obtained from at least three independent assays. ^bN.A.: not active at 10 μM. ^cConcentration in nM.

the fourth series were not toxic in the concentrations tested. Considering the selectivity indexes obtained, 8 and 12 were the most promising candidates for *T. brucei* with more than 60 of predicted SI. For *Leishmania*, the expected SIs are inferior to 10, thus making these molecules of lower interest, with the most promising hit being 8. For malaria, relatively low LD₅₀ and SI values were found for hit compounds 3, 7, and 16 (Table 2).

The calculated SIs for compounds 3, 7, and 16 are between 19 and 70 within the acceptable safety range (SI values greater than 10 indicate that a compound has an acceptable therapeutic window in the development of antimalarial drugs).²⁶

The *in vitro* hemolysis assay evaluates the liberation of hemoglobin in the medium due to the lysis of erythrocytes after exposure to the test compounds. Drug-induced hemolysis can occur by two mechanisms: allergic and toxic hemolysis. The allergic hemolysis refers to toxicity cause by an immunological reaction in people previously sensitized to a drug while the toxic hemolysis is the direct toxicity of the drug, drug metabolites, or an excipient in the formulation.²⁷ This assay was intended to evaluate the potential toxic hemolytic effect of the hit compounds 3, 7, and 16 on healthy/nonparasitized erythrocytes (Figure 3). The percent of hemolysis induced by the compounds was also determined under standard culture conditions of *P. falciparum*. The percent of hemolysis of healthy erythrocytes induced by 3, 7, and 16 was lower than 6% (for all tested concentration 0.04–10 μM; Figure 3) and within the range of that of CQ (for all tested doses). Compounds 3, 7, and 16 and CQ had no hemolytic activity at ≤10 μM (the highest concentration tested for antimalarial activity and much higher than the peak plasma concentration attained during chloroquine treatment of

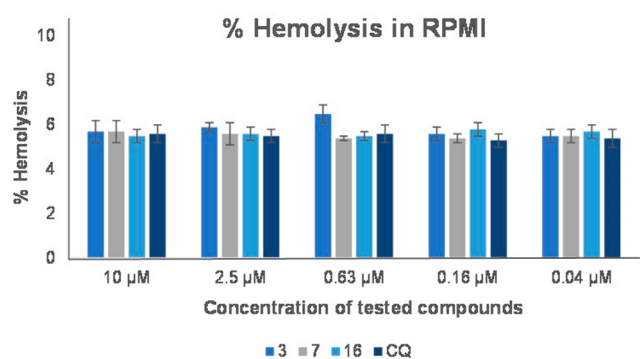


Figure 3. Hemolysis of healthy erythrocytes *in vitro* induced by the compounds. The error bars represent the mean ± standard deviation of % hemolysis of the compounds compared to the positive control obtained by action of Triton X-100.

malaria).²⁸ CQ is considered a nonhemolytic antimalarial drug in healthy human erythrocytes.²⁹ Compounds 3, 7, and 16 did not present hemolytic activity, since the % hemolysis was <10% (% hemolysis > 25% is considered as indicative of risk of hemolysis³⁰).

The evaluation of inhibition of the polymerization of hemozoin (β -hematin) *in vitro* was based on the protocol of Basilio et al.³¹ with some modifications and was carried out for compounds 3, 7, 16, and CQ by using hemin solution (ferriprotoporphyrin IX chloride). CQ was used as a positive control to evaluate the quality of the test since CQ binds to portions of hemozoin produced from the proteolytic process of hemoglobin in infected erythrocytes, thus interfering with hemozoin detoxification. Compounds, 3, 7, and 16 did not show inhibition of the polymerization of β -hematin *in vitro*

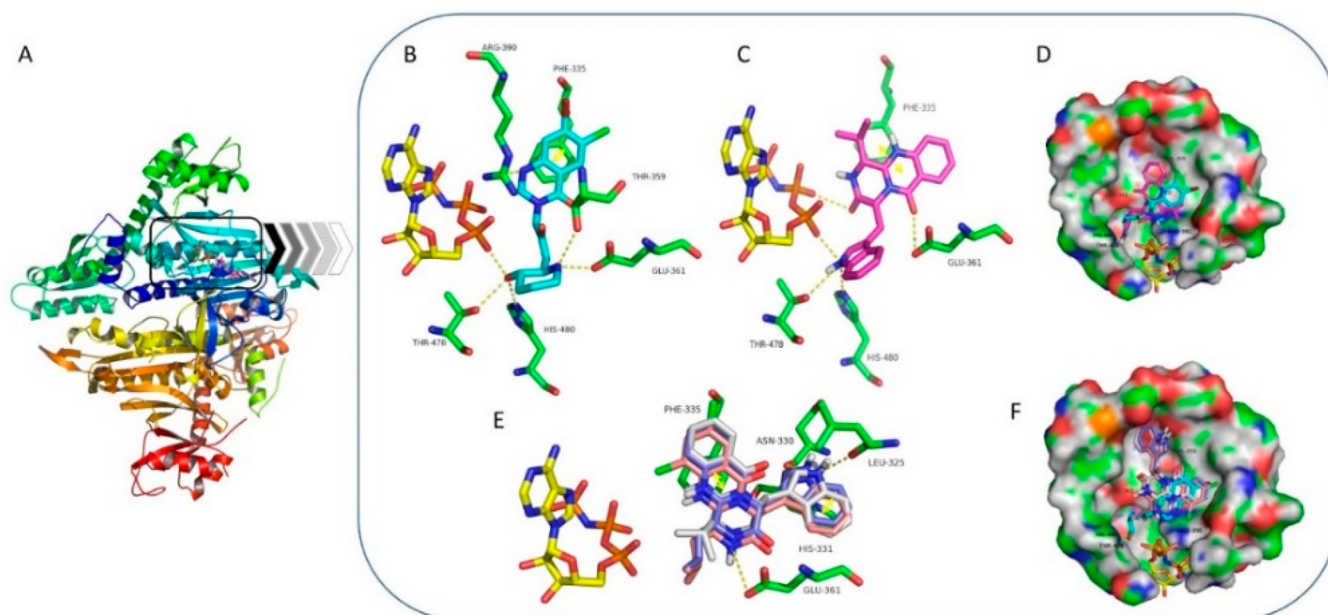


Figure 4. (A) Ribbon representation of *P. falciparum* prolyl-tRNA synthetase (PfPRS) (PDB code: 4YDQ) with crystallographic HF and top scored test molecules. (B) Crystallographic HF (light blue sticks); (C) **4** (pink sticks), (E) **3** (white sticks), **7** (dark blue sticks), and **16** (salmon sticks) docked into the PRD active site. Relevant amino acids are represented as capped sticks and labeled. AMPPNP is represented as yellow sticks. Polar interactions are represented in yellow broken lines. π -Stacking interactions are represented with double arrows. Capped surface representation of PRS with docked conformations of (D) crystallographic HF and **4**, and (F) crystallographic HF, **3**, **7**, and **16**. Some PRS residues are omitted for simplification. AMPPNP = yellow; crystallographic HF = light blue; **4** = pink; **7** = blue; **16** = salmon; **3** = white. Polar interactions are represented by yellow broken lines. On the surface, carbons, oxygens, nitrogens, and hydrogens are represented in green, red, blue, and gray, respectively.

(Supporting Information, Figure S36). Febrifugine significantly inhibits the detoxification of heme by biopolymerization into hemozoin which will not allow the parasites to survive. Even though the indole-containing pyrazino[2,1-*b*]quinazolinone-3,6-dinones **3**, **7**, and **16** possess structure similarities with febrifugine, the results proposed that another mechanism of action for these derivatives should be involved.

The quinazolinone-type alkaloid febrifugine (FF), the active compound of the ancient Chinese herb *Dichroa febrifuga*, and its derivative halofuginone (HF),³² a semisynthetic analogue in clinical trials,³³ have been described as effective treatments for malaria disease.³² Recently, the target of HF was disclosed as prolyl-tRNA synthetase (PRS) enzyme (Figure 4A), a member of the aminoacyl-tRNA synthetase (aaRS) family that drives protein translation.³² Therefore, we hypothesized these compounds could be targeting the malaria protein translation machinery by inhibition of the *P. falciparum* prolyl-tRNA synthetase (PfPRS). Moreover, PRS in *L. infantum* (LiPRS) is also described as a therapeutic target for quinazolinones.³⁴ Since the three-dimensional structure of LiPRS is not available, the homology model was built using the 3D structure of *Leishmania major* PRS (LmPRS) (PDB code 5XIL) as a template (Supporting Information, Figure S37–S39).³⁴ It was selected because it showed the highest percentage similarity (99.2%), the highest percentage identity (97.3%), and the lowest E-value (0.0) (constraint that defines the number of hits one can expect to see by chance when finding it in a molecular database).³⁵ The best model was based on the lowest packing score (2.12) (smaller value means higher probability structure–sequence combination), the lowest contact energy (-385.8 kcal.mol⁻¹), the lowest electrostatic solvation energy

(generalized Born/volume integral GB/VI) (-23 896.0 kcal.mol⁻¹),³⁶ and zero atom clashes.³⁷

Subsequently, docking studies in both PfPRS and LiPRS were performed to comprehend the underlying molecular mode of action of that class of compounds. Positive controls [febrifugine (FF), halofuginone (HF), 6-fluorofebrifugine (6F-FF), and tetrahydroquinazolinone febrifugine (Th-FF)] were predicted as having a high binding affinity to the PRS enzyme target, with docking scores from -9.3 to -9.7 kcal.mol⁻¹ in PfPRS and from -7.9 to -8.2 kcal.mol⁻¹ in LiPRS. The docking scores of all tested compounds range from -7.3 to -11.5 kcal.mol⁻¹ and from -8.0 to -10.5 kcal.mol⁻¹ for PfPRS and LiPRS, respectively (Table 4). The most active antimalarial (compounds **3**, **4**, **7** and **16**) and antileishmania (compounds **8**, **18**, and **19**) agents *in vitro* presented docking scores from -9.1 to -11.4 kcal.mol⁻¹ and from -8.7 to -9.0 kcal.mol⁻¹ for PfPRS and in LiPRS, respectively, therefore being predicted as forming stable complexes with PRS enzymes.

HF is described as being a mimetic of the enzyme-substates L-Pro and adenine-76 of tRNA, binding to the active site compartment simultaneously with ATP.³² In addition to HF, other quinazolinone-based compounds such as FF, 6F-FF, and Th-FF have also been described as specific for PRS, when in the presence of the ATP analogue AMPPNP.³⁸ The structure of the ternary complex of PfPRS-adenosin 5'-(β,γ -imido)-triphosphate (AMPPNP)-HF shows hydrogen interactions with Thr359, Glu361, Arg390, Thr478, and His480 and π -stacking interactions with Phe335³⁸ (Figure 4B). Compound **4** fits the same binding pocket as HF, binding with some of the same residues as HF. The N atom of the indole ring forms hydrogen bonds with Thr478, His480 and with AMPPNP phosphate groups; and the pyrazinoquinazolinone ring is

Table 4. Docking Scores of Test Compounds and Controls onto *P. falciparum* and *L. infantum* PRS Binding Site

test molecule	docking scores (kcal·mol ⁻¹)	
	PfPRS (PDB: 4YDQ)	LiPRS model
1	-10.7	-8.3
2	-8.9	-8
3	-9.1	-9.3
4	-11.4	-8.1
5	-9.9	-8.7
6	-7.8	-9
7	-10	-9.2
8	-11.5	-8.7
9	-10.3	-8.2
12	-7.7	-9.4
13	-7.3	-9.9
14	-9.4	-8.9
15	-7.6	-8.9
16	-9.9	-9
17	-8.9	-9
18	-7.3	-9
19	-8.6	-9
21	-8.3	-10.5
22	-8.4	-8.8
23	-9.7	-9
24	-8.6	-8.9
25	-9.4	-9
26	-10.1	-8.6
27	-7.8	-9.6
FF	-9.5	-7.9
HF	-9.3	-8.2
ThFF	-9.5	-7.8
6F-FF	-9.7	-8.2

mainly stabilized by hydrogen interactions with Glu361 and π -stacking contacts with Phe335 (Figure 4C–D).

The pyrazinoquinazolinone **4** does not establish polar interactions with Arg390, suggesting chemical spaces available for additional modifications or derivatizations. Compounds **3**, **7**, and **16** bind in the same position in the PRS cavity, but they are not predicted to establish hydrogen interactions with AMPPNP. Hydrogen interactions are formed with residues Glu361, Leu325, and Asn330; π -stacking interactions are established with Phe335 and His331 (Figure 4E, F). The indole ring of **3**, **7**, and **16** docks into a lateral cavity flanked by His331, that is not occupied by HF (Figure 4F). The binding pose of **9**, different from the binding poses of **3**, **7**, and **16**, provides a hint on the relevance of chirality in the affinity of the binding to PRS target. The binding pocket in LiPRS is essentially identical (Figure 5A), thus suggesting that the active site for quinazolinone derivatives is the same in different PRS.

The indole groups of **8**, **18**, and **19** establish polar interactions with Ser323; the pyrazinoquinazolinones of **18** and **19** also bind to Glu324 and Ser323; **8** establishes hydrogen interactions with AMPPNP phosphate groups (Figure 5B). The shape of the target active site is narrow, with tight recesses, which will cause steric hindrance if the ligand does not have the appropriate geometry and, thus, a favorable chirality (Figure 6).

In order to better understand what descriptors are crucial for the activity against *P. falciparum* of the tested indole-containing pyrazinoquinazolinone compounds, a quantitative SAR (QSAR) model was built (see the Supporting Information for details).

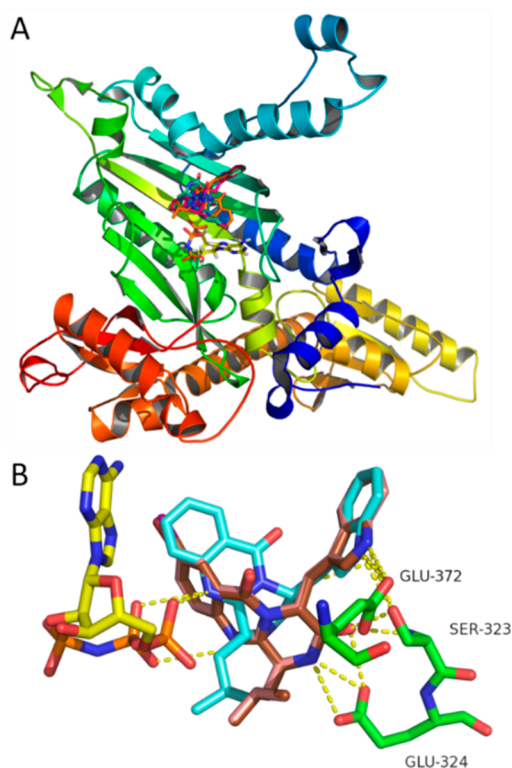


Figure 5. (A) Ribbon representation of *L. infantum* prolyl-tRNA synthetase (LiPRS) model with top scored test molecules. (B) **8** (light blue sticks), **18** (beige sticks), and **24** (brown sticks) on the LiPRS binding site, with relevant amino acids represented as capped sticks and labeled. AMPPNP is represented as yellow sticks. Polar interactions are represented as yellow broken lines.

Thus, a 2D-QSAR model was obtained using Comprehensive Descriptors for Structural and Statistical Analysis (CODESSA 2.7.2) software, and the heuristic method was chosen to perform a preselection of descriptors.³⁹ The correlation coefficient (R^2), squared standard error (S^2), and Fisher's value (F) were used to assess the validity of the regression equation. As the rules of QSAR establish that there must be one descriptor for each of the five molecules used to build the model,⁴⁰ two descriptors were used to build the QSAR equation. The multilinear regression analysis using the heuristic method for 10 compounds in the two-descriptor model is via eq 1.

$$\begin{aligned} \log(1/IC_{50}) (\mu\text{M}) = & 62.063(\pm 18.730)\text{FNSA3} + 12.539(\pm 4.6309) \\ & \times \text{XY-Shadow/XY-Rectangle} - 6.4255(\pm 2.8635) \\ (n = 10; R^2 = 0.7603; S^2 = 0.149; F = 11.10; Q^2 = 0.616) \end{aligned} \quad (1)$$

where FNSA3 means fractional partial negatively charged surface area.

The analysis of the molecular descriptors in the regression model (eq 1) allows the identification of the characteristics that are expected to be responsible for antimalarial activity of the studied compounds. Descriptors which appear in this model are geometric-electronic (FNSA3) and geometrical (XY shadow/XY rectangle), which reveals the role of electronic and steric interactions that affect the antimalarial activity of indole-containing pyrazinoquinazolinones. The FNSA3 fractional charged surface area-type descriptor is important in governing

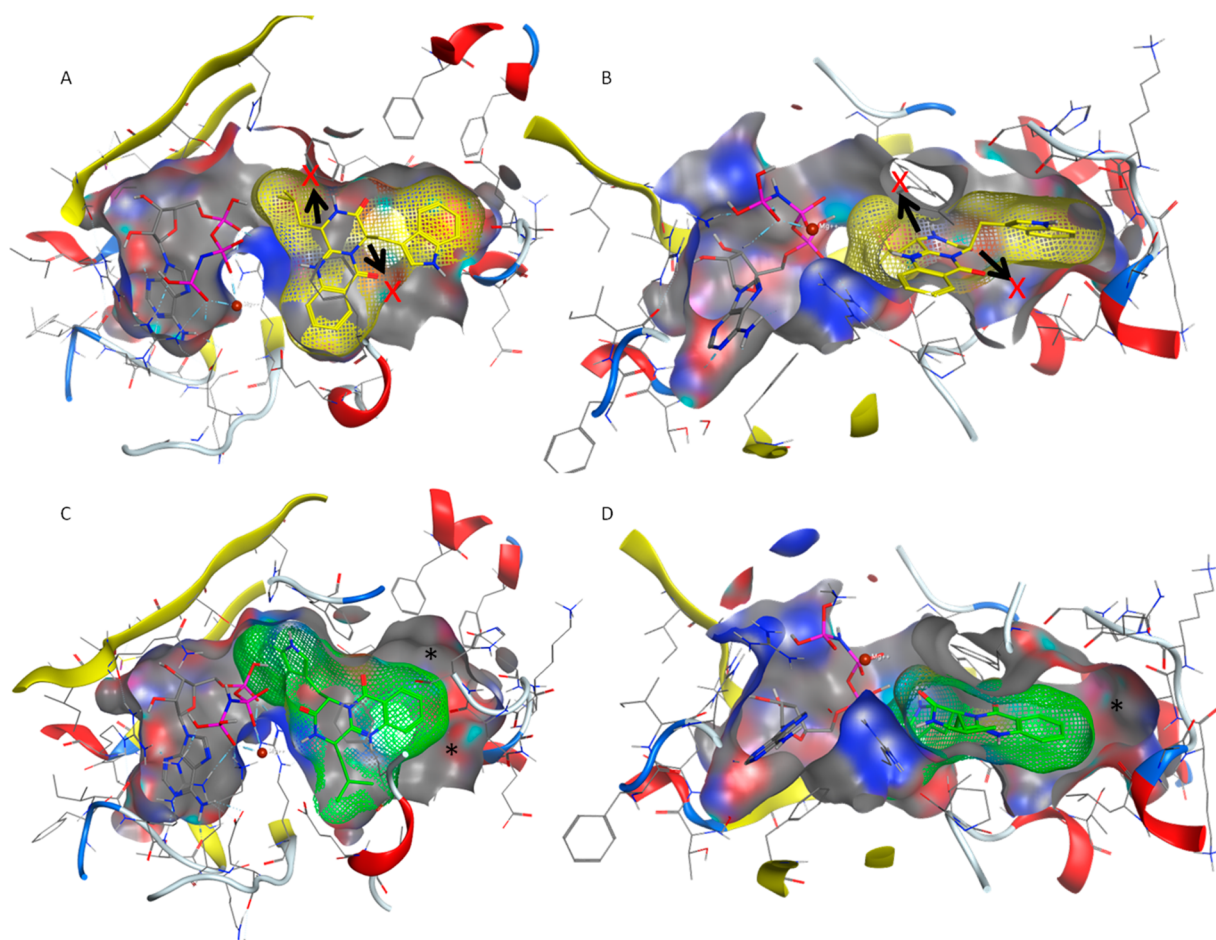


Figure 6. Compound 7 (1*S*,4*R*) (yellow sticks) in top (A) and site (B) view docked onto PfPRS binding site (docking score of -10 kcal·mol $^{-1}$). Compound 6 (1*R*,4*S*) (green sticks) in top (C) and site (D) view docked onto PfPRS binding site (docking score of -7.8 kcal·mol $^{-1}$). The binding site of the receptor is represented as a capped solid gray surface, whereas compound 7 and 6 surfaces are represented as yellow and green meshes, respectively. AMPPNP is represented as gray sticks. The binding pocket and compound 7 (1*S*,4*R*) have perfect steric complementarity (docking score of -10 kcal·mol $^{-1}$). However, if compound 6 (1*R*,4*S*) was placed in the binding pocket in the exact same position, there would be steric clashes between the 1-*t*-butyl and 4-indol groups in the ligand and the receptor atoms (as represented by the black arrows). Thus, compound 6 will dock in a different and less favorable pose (docking score of -7.8 kcal·mol $^{-1}$) as seen by the empty space left in the target cavity (*). Also, compound 7 docks in such a conformation that maximizes electrostatic interactions, such as π -stacking with Phe-335 or hydrogen interaction with Asn-330 (Figure 4E). Such interactions are missed by compound 6. Each enantiomeric pair behaves differently, and here compounds 6 and 7 are used as examples to illustrate the importance of chirality.

the QSAR model with its high *t*-criterion (3.313). FNSA3 is the atomic charge weighted negative surface area (PNSA3) divided by the total molecular solvent-accessible surface area (TMSA), *i.e.*, PNSA3/TMSA. This descriptor is calculated by mapping atomic partial charges on the solvent-accessible surface areas of individual atoms, meaning that shape and electronic characteristics of the molecule are relevant for activity.⁴¹ The second largest contributing molecular descriptor is *XY*-Shadow/*XY*-Rectangle, which is a geometrical descriptor, related on size and shape of molecules in terms of its 3D coordinates. This descriptor represents a two-dimensional projection on the *X*–*Y* plane of a three-dimensional molecule. A positive sign means that the activity increases with increasing the value of *XY* shadow, which means that a higher area of molecular shadow in the enclosing rectangle will benefit the activity.⁴² The examination of the molecular descriptors led to a better understanding of the relation between structure and antimalarial activity. Electronic and geometric properties seem to be important for the activity of indole-containing pyrazinoquinazolines. As chiral atoms

affect the overall geometry, chirality will probably also affect antimalarial activity.

In conclusion, the indole-containing pyrazino[2,1-*b*]-quinazoline-3,6-dinone scaffold was discovered as a remarkable source of species-specific bioactive molecules against relevant parasites. Subtle modifications at the C-1 position and the introduction of halogens are allowed, but ring A isosteres were detrimental for antiparasitic activity. The hit compounds that disclosed activity against the one (7, *P. falciparum*) or three pathogens (8, *P. falciparum*, *T. brucei* and *L. infantum*) did not show significant hemolytic activity in healthy human erythrocytes or inhibit β -hematin *in vitro*. *In silico* molecular studies predicted prolyl-tRNA as a molecular target of these compounds similarly to halofuginone and paved the way to future molecular optimizations. Indole-containing pyrazino[2,1-*b*]quinazoline-3,6-dinone derivatives are herein disclosed to have antiparasitic activity, and these findings support the potential of quinazolinones for the development of new antiprotozoan drugs in medicinal chemistry.

■ ASSOCIATED CONTENT

SI Supporting Information

The Supporting Information is available free of charge at <https://pubs.acs.org/doi/10.1021/acsmchemlett.1c00589>.

Additional experimental details, materials, and methods, synthetic procedures, compound characterization (^1H , ^{13}C NMR and HMBC spectra for all compounds, as well as high resolution mass spectrometry) and enantioselective liquid chromatography; biological activity additional experimental details and computational docking studies details (PDF)

■ AUTHOR INFORMATION

Corresponding Authors

Fátima Nogueira – *Global Health and Tropical Medicine (GHTM), Instituto de Higiene e Medicina Tropical, IHMT, Universidade Nova de Lisboa, 1349-008 Lisboa, Portugal;* orcid.org/0000-0003-0313-0778; Phone: +351 213652600; Email: fnogueira@ihmt.unl.pt

Emília Sousa – *Laboratório de Química Orgânica e Farmacêutica, Faculdade de Farmácia, Universidade do Porto, 4050-313 Porto, Portugal; CIIMAR - Centro Interdisciplinar de Investigação Marinha e Ambiental, 4450-208 Matosinhos, Portugal;* orcid.org/0000-0002-5397-4672; Phone: +351-220428689; Email: esousa@ff.up.pt

Authors

Solida Long – *Laboratório de Química Orgânica e Farmacêutica, Faculdade de Farmácia, Universidade do Porto, 4050-313 Porto, Portugal; Department of Bioengineering, Royal University of Phnom Penh, 12156 Phnom Penh, Cambodia*

Denise Duarte – *Global Health and Tropical Medicine (GHTM), Instituto de Higiene e Medicina Tropical, IHMT, Universidade Nova de Lisboa, 1349-008 Lisboa, Portugal*

Carla Carvalho – *Parasite Disease Group, IBMC-Instituto de Biologia Molecular e Celular, 4200-135 Porto, Portugal*

Rafael Oliveira – *Global Health and Tropical Medicine (GHTM), Instituto de Higiene e Medicina Tropical, IHMT, Universidade Nova de Lisboa, 1349-008 Lisboa, Portugal*

Nuno Santarém – *Parasite Disease Group, IBMC-Instituto de Biologia Molecular e Celular, 4200-135 Porto, Portugal*

Andreia Palmeira – *Laboratório de Química Orgânica e Farmacêutica, Faculdade de Farmácia, Universidade do Porto, 4050-313 Porto, Portugal; CIIMAR - Centro Interdisciplinar de Investigação Marinha e Ambiental, 4450-208 Matosinhos, Portugal*

Diana I. S. P. Resende – *Laboratório de Química Orgânica e Farmacêutica, Faculdade de Farmácia, Universidade do Porto, 4050-313 Porto, Portugal; CIIMAR - Centro Interdisciplinar de Investigação Marinha e Ambiental, 4450-208 Matosinhos, Portugal*

Artur M. S. Silva – *QOPNA - Química Orgânica, Produtos Naturais e Agroalimentares, Departamento de Química, Universidade de Aveiro, 3810-193 Aveiro, Portugal;* orcid.org/0000-0003-2861-8286

Rui Moreira – *Research Institute for Medicines and Pharmaceutical Sciences (iMed.UL), Faculdade de Farmácia, Universidade de Lisboa, 1649-019 Lisboa, Portugal;* orcid.org/0000-0003-0727-9852

Anake Kijjoa – *CIIMAR - Centro Interdisciplinar de Investigação Marinha e Ambiental, 4450-208 Matosinhos,*

Portugal; ICBAS-Instituto de Ciências Biomédicas Abel Salazar, Universidade do Porto, 4050-313 Porto, Portugal
Anabela Cordeiro da Silva – *Parasite Disease Group, IBMC-Instituto de Biologia Molecular e Celular, 4200-135 Porto, Portugal; Departamento de Ciências Biológicas, Faculdade de Farmácia, Universidade do Porto, 4050-313 Porto, Portugal*
Madalena M. M. Pinto – *Laboratório de Química Orgânica e Farmacêutica, Faculdade de Farmácia, Universidade do Porto, 4050-313 Porto, Portugal; CIIMAR - Centro Interdisciplinar de Investigação Marinha e Ambiental, 4450-208 Matosinhos, Portugal*

Complete contact information is available at: <https://pubs.acs.org/doi/10.1021/acsmchemlett.1c00589>

Author Contributions

E.S. and A.K. conceived the study design. S.L. synthesized the compounds and elucidated their structure, and A.M.S.S., E.S., and M.M.M.P. analyzed the data. D.I.S.P.R. performed the HPLC analysis. A.P. and N.S. performed the in silico study. F.N. conceived the *P. falciparum* susceptibility assays and discussed and wrote the results, while D.D. and R.O. performed those studies. A.C.S. conceived the *Leishmania*, *T. brucei*, and THP1 studies. C.C. performed the in vitro assays for *Leishmania*, *T. brucei*, and THP1. N.S. analyzed the data, wrote the manuscript, and conceived the *Leishmania*, *T. brucei*, and THP1 studies. S.L. and E.S. wrote the manuscript, while all authors gave significant contributions in discussion and revision. All authors agreed to the final version of the manuscript.

Funding

This research was supported by national funds through FCT-Foundation for Science and Technology within the scope of UIDB/04423/2020, UIDP/04423/2020, IUD/04413/2020 and under the project PTDC/SAU-PUB/287336/2017 (reference POCI-01-0145-FEDER-028736), cofinanced by COMPETE 2020, Portugal 2020 and the European Union through the ERDF and by FCT through national funds, as well as CHIRALBIOACTIVE-PI-3RL-IINFACETS-2019. This work is a result of the project ATLANTIDA (reference NORTE-01-0145-FEDER-000040), supported by the Norte Portugal Regional Operational Programme (NORTE 2020), under the PORTUGAL 2020 Partnership Agreement and through the European Regional Development Fund (ERDF). The work was also funded by FEDER-Fundo Europeu de Desenvolvimento Regional through COMPETE 2020-Programa Operacional para a Competitividade e Internacionalização (POCI), Portugal 2020, and by Portuguese fundings through (FCT-Fundação para a Ciência e a Tecnologia/Ministério da Ciência, Tecnologia e Inovação, under the project “Instituto de Investigação e Inovação em Ciências da Saúde” “(POCI-01-0145-FEDER-007274)”. N.S. and C.C. are supported by Fundação e Ciência (MEC) cofunded by FEDER through the COMPETE 2020 Operational Programme for Competitiveness and Internationalisation (POCI) referent POCI-01-0145-FEDER-031013. S.L. is thankful to Erasmus Mundus Action 2 (LOTUS+ LP15DF0205) for a full PhD scholarship and HEIP-RUPP-SGA-11 project. The authors thank Sara Cravo for technical support.

Notes

The authors declare no competing financial interest.

■ ABBREVIATIONS AND ACRONYMS

6F-FF, 6-fluorofebifugine; aaRS, aminoacyl-tRNA synthetase; ACTs, artemisinin combination therapies; AMPNP, adenosine 5'-(β,γ -imido)triphosphate; Boc, *tert*-butyloxycarbonyl; CL, cutaneous leishmaniasis; compds, compounds; CQ, chloroquine; FF, febrifugine; GB, generalized Borna disease; GMS, Greater Mekong Subregion; HAT, human African trypanosomiasis; HF, halofuginone; HPLC, high performance liquid chromatography; LiPRS, *L. infantum* Prolyl-tRNA synthetase; LmPRS, *Leishmania major* prolyl-tRNA synthetase; ML, mucocutaneous leishmaniasis; MTT, methyl thiazolyl diphenyl-tetrazolium bromide; ND, neglected diseases; PpPRS, *P. falciparum* prolyl-tRNA synthetase; PRS, prolyl-tRNA synthetase; SD, standard deviation; SI, selectivity index; TCAMS, Tres Cantos Antimalarial Set; Th-FF, tetrahydroquinazolinone febrifugine; VI, volume integral; VL, visceral leishmaniasis; WHO, World Health Organization

■ REFERENCES

- (1) World Health Organization. *Global technical strategy for malaria 2016–2030, 2021 update*; World Health Organization: Geneva, 2021.
- (2) World Health Organization. Leishmaniasis. <http://www.who.int/leishmaniasis/en/> (accessed 2021-12-28).
- (3) World Health Organization. *Control and surveillance of human African trypanosomiasis: Report of a WHO expert committee*; World Health Organization: Geneva, 2013.
- (4) World Health Organization. *World malaria report 2021*; World Health Organization: Geneva, 2021.
- (5) Nogueira, F.; Rosário, V. E. d. Methods for assessment of antimalarial activity in the different phases of the *Plasmodium* life cycle. *Rev. Pan-Amaz. Saude* **2010**, *1*, 109–124.
- (6) Calderaro, A.; Piccolo, G.; Gorrini, C.; Rossi, S.; Montecchini, S.; Dell'Anna, M. L.; De Conto, F.; Medici, M. C.; Chezzi, C.; Arcangeletti, M. C. Accurate identification of the six human *Plasmodium* spp. causing imported malaria, including *Plasmodium ovale wallikeri* and *Plasmodium knowlesi*. *Malar. J.* **2013**, *12* (1), 321.
- (7) Petersen, I.; Eastman, R.; Lanzer, M. Drug-resistant malaria: Molecular mechanisms and implications for public health. *FEBS Lett.* **2011**, *585* (11), 1551–1562.
- (8) Zheng, C.-J.; Li, L.; Zou, J.-p.; Han, T.; Qin, L.-P. Identification of a quinazolinone alkaloid produced by *Penicillium vinaceum*, an endophytic fungus from *Crocus sativus*. *Pharm. Biol.* **2012**, *50* (2), 129–133.
- (9) Fernández-Álvarez, E.; Hong, W. D.; Nixon, G. L.; O'Neill, P. M.; Calderón, F. Antimalarial Chemotherapy: Natural Product Inspired Development of Preclinical and Clinical Candidates with Diverse Mechanisms of Action. *J. Med. Chem.* **2016**, *59* (12), 5587–5603.
- (10) Oliveira, R.; Guedes, R. C.; Meireles, P.; Albuquerque, I. S.; Gonçalves, L. M.; Pires, E.; Bronze, M. R.; Gut, J.; Rosenthal, P. J.; Prudêncio, M.; Moreira, R.; O'Neill, P. M.; Lopes, F. Tetraoxane-pyrimidine nitrile hybrids as dual stage antimalarials. *J. Med. Chem.* **2014**, *57* (11), 4916–4923.
- (11) Flannery, E. L.; Chatterjee, A. K.; Winzeler, E. A. Antimalarial drug discovery—approaches and progress towards new medicines. *Nat. Rev. Microbiol.* **2013**, *11* (12), 849–862.
- (12) Almela, M. J.; Lozano, S.; Lelièvre, J.; Colmenarejo, G.; Coterón, J. M.; Rodrigues, J.; Gonzalez, C.; Herreros, E. A New Set of Chemical Starting Points with *Plasmodium falciparum* Transmission-Blocking Potential for Antimalarial Drug Discovery. *PLoS One* **2015**, *10* (8), e0135139.
- (13) Rottmann, M.; McNamara, C.; Yeung, B. K. S.; Lee, M. C. S.; Zou, B.; Russell, B.; Seitz, P.; Plouffe, D. M.; Dharia, N. V.; Tan, J.; Cohen, S. B.; Spencer, K. R.; González-Páez, G. E.; Lakshminarayana, S. B.; Goh, A.; Suwanarusk, R.; Jegla, T.; Schmitt, E. K.; Beck, H. P.; Brun, R.; Nosten, F.; Renia, L.; Dartois, V.; Keller, T. H.; Fidock, D. A.; Winzeler, E. A.; Diagona, T. T. Spiroindolones, a potent compound class for the treatment of malaria. *Science* **2010**, *329* (5996), 1175–1180.
- (14) Barker, R. H., Jr; Urgaonkar, S.; Mazitschek, R.; Celatka, C.; Skerlj, R.; Cortese, J. F.; Tyndall, E.; Liu, H.; Cromwell, M.; Sidhu, A. B.; Guerrero-Bravo, J. E.; Crespo-Llado, K. N.; Serrano, A. E.; Lin, J. W.; Janse, C. J.; Khan, S. M.; Duraisingh, M.; Coleman, B. I.; Angulo-Barturen, I.; Jiménez-Díaz, M. B.; Magán, N.; Gomez, V.; Ferrer, S.; Martínez, M. S.; Wittlin, S.; Papastogiannidis, P.; O'Shea, T.; Klinger, J. D.; Bree, M.; Lee, E.; Levine, M.; Wiegand, R. C.; Munoz, B.; Wirth, D. F.; Clardy, J.; Bathurst, I.; Sybertz, E. Aminindoles, a novel scaffold with potent activity against *Plasmodium falciparum*. *Antimicrob. Agents Chemother.* **2011**, *55* (6), 2612–2622.
- (15) Gamó, F. J.; Sanz, L. M.; Vidal, J.; De Cozar, C.; Alvarez, E.; Lavandera, J. L.; Vanderwall, D. E.; Green, D. V. S.; Kumar, V.; Hasan, S.; Brown, J. R.; Peishoff, C. E.; Cardon, L. R.; Garcia-Bustos, J. F. Thousands of chemical starting points for antimalarial lead identification. *Nature* **2010**, *465* (7296), 305–310.
- (16) Resende, D. I. S. P.; Boonpothong, P.; Sousa, E.; Kijjoo, A.; Pinto, M. M. M. Chemistry of the fumiquinazolines and structurally related alkaloids. *Nat. Prod. Rep.* **2019**, *36*, 7–34.
- (17) Long, S.; Furlani, I. L.; Oliveira, J. M. d.; Resende, D. I. S. P.; Silva, A. M. S.; Gales, L.; Pereira, J. A.; Kijjoo, A.; Cass, Q. B.; Oliveira, R. V.; Sousa, E.; Pinto, M. M. M. Determination of the Absolute Configuration of Bioactive Indole-Containing Pyrazino[2,1-b]-quinazolinone-3,6-diones and Study of Their In Vitro Metabolic Profile. *Molecules* **2021**, *26* (16), 5070.
- (18) Long, S.; Resende, D. I. S. P.; Kijjoo, A.; Silva, A. M. S.; Pina, A.; Fernández-Marcelo, T.; Vasconcelos, M. H.; Sousa, E.; Pinto, M. M. M. Antitumor Activity of Quinazolinone Alkaloids Inspired by Marine Natural Products. *Mar. Drugs* **2018**, *16* (8), 261.
- (19) Long, S.; Resende, D. I. S. P.; Kijjoo, A.; Silva, A. M. S.; Fernandes, R.; Xavier, C. P. R.; Vasconcelos, M. H.; Sousa, E.; Pinto, M. M. M. Synthesis of New Proteomimetic Quinazolinone Alkaloids and Evaluation of Their Neuroprotective and Antitumor Effects. *Molecules* **2019**, *24* (3), 534.
- (20) Long, S.; Resende, D. I. S. P.; Palmeira, A.; Kijjoo, A.; Silva, A. M. S.; Tiritan, M. E.; Pereira-Terra, P.; Freitas-Silva, J.; Barreiro, S.; Silva, R.; Remião, F.; Pinto, E.; Martins da Costa, P.; Sousa, E.; Pinto, M. M. M. New marine-derived indolymethyl pyrazinoquinazolinone alkaloids with promising antimicrobial profiles. *RSC Adv.* **2020**, *10* (52), 31187–31204.
- (21) Liu, J.-F.; Lee, J.; Dalton, A. M.; Bi, G.; Yu, L.; Baldino, C. M.; McElory, E.; Brown, M. Microwave-assisted one-pot synthesis of 2,3-disubstituted 3H-quinazolin-4-ones. *Tetrahedron Lett.* **2005**, *46* (8), 1241–1244.
- (22) Pathak, M.; Ojha, H.; Tiwari, A. K.; Sharma, D.; Saini, M.; Kakkar, R. Design, synthesis and biological evaluation of antimalarial activity of new derivatives of 2,4,6-s-triazine. *Chem. Cent. J.* **2017**, *11* (1), 132–132.
- (23) Zhu, S.; Wang, J.; Chandrashekar, G.; Smith, E.; Liu, X.; Zhang, Y. Synthesis and evaluation of 4-quinazolinone compounds as potential antimalarial agents. *Eur. J. Med. Chem.* **2010**, *45* (9), 3864–3869.
- (24) Zhu, S.; Meng, L.; Zhang, Q.; Wei, L. Synthesis and evaluation of febrifugine analogues as potential antimalarial agents. *Bioorg. Med. Chem. Lett.* **2006**, *16* (7), 1854–1858.
- (25) Villarreal, W.; Colina-Vegas, L.; Rodrigues de Oliveira, C.; Tenorio, J. C.; Ellena, J.; Gozzo, F. C.; Cominetti, M. R.; Ferreira, A. G.; Ferreira, M. A. B.; Navarro, M.; Batista, A. A. Chiral Platinum(II) Complexes Featuring Phosphine and Chloroquine Ligands as Cytotoxic and Monofunctional DNA-Binding Agents. *Inorg. Chem.* **2015**, *54* (24), 11709–11720.
- (26) Katsuno, K.; Burrows, J. N.; Duncan, K.; Van Huijsduijnen, R. H.; Kaneko, T.; Kita, K.; Mowbray, C. E.; Schmatz, D.; Warner, P.; Slingsby, B. T. Hit and lead criteria in drug discovery for infectious diseases of the developing world. *Nat. Rev. Drug Discovery* **2015**, *14* (11), 751–758.
- (27) Dausset, J.; Contu, L. Drug-Induced Hemolysis. *Annu. Rev. Med.* **1967**, *18* (1), 55–70.

(28) Mesa-Echeverry, E.; Niebles-Bolívar, M.; Tobón-Castaño, A. Chloroquine–Primaquine Therapeutic Efficacy, Safety, and Plasma Levels in Patients with Uncomplicated Plasmodium vivax Malaria in a Colombian Pacific Region. *American Journal of Tropical Medicine and Hygiene* **2019**, *100* (1), 72–77.

(29) Chou, A. C.; Fitch, C. D. Hemolysis of mouse erythrocytes by ferriprotoporphyrin IX and chloroquine. Chemotherapeutic implications. *J. Clin. Investig* **1980**, *66* (4), 856–858.

(30) Amin, K.; Dannenfelser, R. M. In vitro hemolysis: Guidance for the pharmaceutical scientist. *J. Pharm. Sci.* **2006**, *95* (6), 1173–1176.

(31) Basilio, N.; Pagani, E.; Monti, D.; Olliaro, P.; Taramelli, D. A microtitre-based method for measuring the haem polymerization inhibitory activity (HPIA) of antimalarial drugs. *J. Antimicrob. Chemother.* **1998**, *42* (1), 55–60.

(32) Keller, T. L.; Zocco, D.; Sundrud, M. S.; Hendrick, M.; Edenius, M.; Yum, J.; Kim, Y. J.; Lee, H. K.; Cortese, J. F.; Wirth, D. F.; Dignam, J. D.; Rao, A.; Yeo, C. Y.; Mazitschek, R.; Whitman, M. Halofuginone and other febrifugine derivatives inhibit prolyl-tRNA synthetase. *Nat. Chem. Biol.* **2012**, *8* (3), 311–7.

(33) Herman, J. D.; Pepper, L. R.; Cortese, J. F.; Estiu, G.; Galinsky, K.; Zuzarte-Luis, V.; Derbyshire, E. R.; Ribacke, U.; Lukens, A. K.; Santos, S. A.; Patel, V.; Clish, C. B.; Sullivan, W. J.; Zhou, H.; Bopp, S. E.; Schimmel, P.; Lindquist, S.; Clardy, J.; Mota, M. M.; Keller, T. L.; Whitman, M.; Wiest, O.; Wirth, D. F.; Mazitschek, R. The cytoplasmic prolyl-tRNA synthetase of the malaria parasite is a dual-stage target of febrifugine and its analogs. *Sci. Transl. Med.* **2015**, *7* (288), 288ra77.

(34) Jain, V.; Yogavel, M.; Kikuchi, H.; Oshima, Y.; Hariguchi, N.; Matsumoto, M.; Goel, P.; Touquet, B.; Jumaní, R. S.; Tacchini-Cottier, F.; Harlos, K.; Huston, C. D.; Hakimi, M. A.; Sharma, A. Targeting Prolyl-tRNA Synthetase to Accelerate Drug Discovery against Malaria, Leishmaniasis, Toxoplasmosis, Cryptosporidiosis, and Coccidiosis. *Structure* **2017**, *25* (10), 1495–1505e6.

(35) Kerfeld, C. A.; Scott, K. M. Using BLAST to teach “E-value-utionary” concepts. *PLoS Biol.* **2011**, *9* (2), e1001014.

(36) Labute, P. The generalized Born/volume integral implicit solvent model: estimation of the free energy of hydration using London dispersion instead of atomic surface area. *Journal of computational chemistry* **2008**, *29* (10), 1693–8.

(37) Vyas, V. K.; Ukawala, R. D.; Ghate, M.; Chintha, C. Homology modeling a fast tool for drug discovery: current perspectives. *Indian J. Pharm. Sci.* **2012**, *74* (1), 1–17.

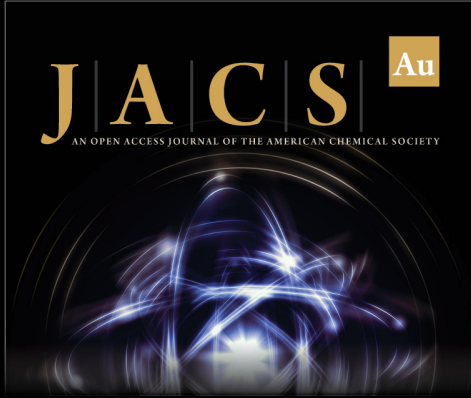
(38) Jain, V.; Yogavel, M.; Oshima, Y.; Kikuchi, H.; Touquet, B.; Hakimi, M. A.; Sharma, A. Structure of Prolyl-tRNA Synthetase-Halofuginone Complex Provides Basis for Development of Drugs against Malaria and Toxoplasmosis. *Structure* **2015**, *23* (5), 819–829.

(39) Liu, P.; Long, W. Current Mathematical Methods Used in QSAR/QSPR Studies. *International Journal of Molecular Sciences* **2009**, *10* (5), 1978–1998.

(40) Kubinyi, H. *QSAR: Hansch Analysis and Related Approaches*; VCH Verlagsgesellschaft mbH: Weinheim, 1993.


(41) Roy, K.; Kar, S.; Das, R. N. *Understanding the Basics of QSAR for Applications in Pharmaceutical Sciences and Risk Assessment*; Academic Press: Boston, 2015; p v.


(42) Todeschini, R.; Consonni, V. *Handbook of Molecular Descriptors*; WILEY-VCH Verlag GmbH: Weinheim, 2000.



JACS Au
AN OPEN ACCESS JOURNAL OF THE AMERICAN CHEMICAL SOCIETY

Editor-in-Chief
Prof. Christopher W. Jones
Georgia Institute of Technology, USA

Open for Submissions 

pubs.acs.org/jacsau  ACS Publications
Most Trusted. Most Cited. Most Read.